*J. Fluid Mech.* (1975), *vol.* 71, *part* 3, *pp.* 577–599
*Printed in Great Britain*



# Forces on bodies moving transversely through a rotating fluid

By P. J. MASON

Geophysical Fluid Dynamics Laboratory, Meteorological Office, Bracknell, Berkshire, England

(Received 13 July 1974 and in revised form 7 May 1975)

Measurements have been made of the net force **F** acting on a bluff rigid body moving with velocity **U** (relative to a fluid rotating about a vertical axis with uniform angular velocity **Ω**) in a plane perpendicular to the axis of rotation. The force **F** is of magnitude $2\Omega\rho VU$, where $\rho$ is the density of the fluid and $V$ is a volume which depends on the size and shape of the body. The relative direction of **F** and **U** is found to depend on the quantity

$$\mathscr{S} \equiv \frac{2\Omega L}{U}\left(\frac{h}{D}\right),$$

where $L$ and $h$ are horizontal and vertical lengths characterizing the object and $D$ is the depth of the fluid in which the object is placed.

## 1. Introduction

A problem of general interest is the determination of the net forces acting on bodies moving through a rotating fluid. Interest in these forces was shown by Taylor (1923), who predicted theoretically, and verified by experiment, a simple but striking result: in a fluid rotating about a vertical axis the force exerted by the fluid on any object moving horizontally about which the fluid motion should be horizontal, such as an upright cylinder, is equal and opposite to the Coriolis force on a mass of fluid with the same volume as the object. Thus if the object has the same density as the fluid, as it did in Taylor's experiment, it moves through the fluid exactly as if the system were not rotating. The Coriolis force on the object is exactly balanced by the force of the fluid. On the other hand Taylor found that an object about which the motion was three dimensional, such as a sphere, was deflected by the Coriolis force.

For Rossby numbers ($R = U/\Omega L$, where $U$ is the flow speed, $\Omega$ the rotation speed and $L$ a typical horizontal length) smaller than those used by Taylor in the aforementioned experiment the constraint of rotation forces the motion about the sphere to be two-dimensional (the Taylor–Proudman theorem: Proudman 1916; Taylor 1923). The flow past the object can then be divided into two regions separated by an imaginary cylinder, with axis parallel to the axis of rotation, which circumscribes the object. Outside this cylinder (a 'Taylor column') the flow behaves as if it were encountering a solid cylinder.

Following the work of Taylor and Proudman a number of theoretical studies of the effect of rapid rotation on transverse flow past objects have been made (e.g. Grace 1926; Stewartson 1953, 1967; Hide 1961; Jacobs 1964; Moore & Saffman 1969). Of particular interest here are those studies which have calculated the net force on the object. These theories, which all assume that the Rossby number is very small, differ in whether the fluid is bounded or unbounded and whether the flow is steady and viscous or unsteady and inviscid.

Stewartson (1953) considered the flow produced by impulsively starting an ellipsoid from rest into steady motion. The fluid was inviscid and unbounded and the Rossby number zero. As the length $c$ of the vertical axis of the ellipsoid increased from zero the ultimate force $F_N$ on the ellipsoid at right angles to the direction of motion and in the opposite direction to the Coriolis force was found to increase from zero to Taylor's two-dimensional value $G$ ($= 2\Omega\rho U V$, where $\rho$ is the density of the fluid and $V$ the volume of the object). This force showed only a weak dependence on the ratio of the horizontal axes of the ellipsoid. The dissipative force $F_T$ in the direction opposite to that of the motion showed a stronger dependence on the horizontal dimensions of the ellipsoid. If $a$ is the length of the ellipsoid axis in the direction of motion and $b$ is the length of the horizontal axis at right angles to this, the force $F_T$ increased with $b/a$ (see figure 11). This force also depended on the length $c$ of the vertical axis and was small for small and large $c$, having a maximum value when $c/(ab)^{\frac{1}{2}} \sim 1$ (see figure 11). In the case of a sphere $F_N = 0{\cdot}38G$ and $F_T = 0{\cdot}49G$.

Using a similar approach Stewartson (1967) considered the motion of a sphere in a fluid between two horizontal planes. The fluid was inviscid and the Rossby number zero. The Taylor-column flow pattern he obtained is identical to that found by Jacobs in a geometrically similar problem which, unlike Stewartson's, was dominated by viscosity. In this case Stewartson found the ultimate force to be equal to that occurring with an object about which the flow is two-dimensional, i.e. $F_T = 0$, $F_N = G$.

Other theories (Moore & Saffman 1969; Wilcox 1972) consider the steady motion of thin disks through a viscous fluid contained between two horizontal planes. The drag on the disk is found to be viscous and due to Ekman-layer stress.

In comparing the experimental results with these theories it will clearly be necessary to determine whether or not the flow gives rise to a Taylor column. Fortunately previous work on Taylor columns gives some insight into this. Hide (1961) has proposed a criterion depending on the change in vorticity necessary for a filament to cross the object and the vorticity of the basic flow. A Taylor column should form for an object of width $L$ in a fluid of depth $D$ if the typical height of the object is greater than $h_c$, where $h_c \sim DU/L\Omega$.

Most of the previous laboratory experiments (Hide & Ibbetson 1966; Hide, Ibbetson & Lighthill 1968; Vaziri & Boyer 1971; Davies 1972) have concentrated on the form of the flow rather than the criterion for the change in flow type. However, these experiments (in particular Hide & Ibbetson 1966) demonstrate that Hide's criterion is important and suggest that a Taylor column forms when $\mathscr{S} \equiv 2\Omega Lh/DU$ is in the range 1–100.

In what follows, the results of two different experiments are presented. In the first experiment a pendulum arrangement is used to measure the net force **F** acting on an object moving through a rotating fluid. This experiment provides a fairly direct measure of the force, but is limited inasmuch as the object has to be a spheroid. The second experiment uses a spinning-disk arrangement which in essence compares the drag force acting on the object with the drag force due to an Ekman layer. This experiment has no restriction on the shape of the object but has the drawback of giving only an indirect and more uncertain measure of the drag force with no information on the sideways or lift forces.

The most straightforward result of the experiments confirms the results of Stewartson's (1967) theory. When the motion is sufficiently slow for a Taylor column to form the dissipative or drag force $F_T$ is very small, being roughly equal in size to an order-of-magnitude estimate of the viscous forces, which were, by design, otherwise negligible in the present experiments. The sideways or 'lift' force $F_N$ equals $G$, i.e. the object is subject to a force equal and opposite to the Coriolis force acting on a mass of fluid with the same volume as the object. Thus, had Taylor (1923) in his experiments with a cylinder and sphere (of density equal to the fluid) moved his sphere *very* slowly through the fluid, then, like the cylinder, it would have been undeflected by the Coriolis force.

At velocities higher than those at which a Taylor column forms both the drag force $F_T$ and lift force $F_N$ are comparable to, but less than, $G$. Thus the reduction in $F_T$ and increase in $F_N$ provide an objective criterion for the occurrence of a Taylor column. The present results agree with previous work in indicating that Hide's criterion $h_c \sim DU/L\Omega$ is appropriate.

The ratio of the non-rotating drag force $\frac{1}{2}\rho A U^2$ (where $A$ is the area of the object in a plane perpendicular to **U**) to the typical size of the 'rotating' drag force $G$ is $\frac{3}{16}R$ in the case of a sphere. Thus, for Rossby numbers of unity and less, the rotating drag force dominates and the experiments show that, provided a Taylor column does not form, this drag force $F_T$ scaled in terms of $G$ is constant. In the case of a sphere, $F_T \sim 0{\cdot}5$ and the lift force $F_N$ is close to zero unless the parameters approach a combination giving Taylor-column formation.

The drag and lift forces are influenced by the shape of the object. The dependence of the lift force on the horizontal aspect ratio of the object (cf. reference to Stewartson 1953 above) was not investigated since only objects with $a = b$ could be used in the 'pendulum' experiments. The lift force was found to increase with $c$ and, in agreement with Taylor's experiment, when $c$ was close to the depth of the container the lift force was $G$ for all Rossby numbers. The drag force depended on $c$ to a lesser degree and was small for small $c$, but unfortunately the measurements at large $c$ were confused by Taylor-column formation. The drag force showed a strong dependence on $b/a$ and $F_T$ was found to be roughly equal to $0{\cdot}5\, G\, b/a$ for $c/(ab)^{\frac{1}{2}} \sim 1$.

Such drag forces comparable with $G$ were first observed in experiments on 'spin-up' in non-axisymmetric containers (Collier & Hide, private communication). Apart from their intrinsic interest these forces are potentially important in geophysical phenomena. There are no theories which have direct relevance to the parameter range of the experiments for which a drag force $\sim G$ occurs. However,

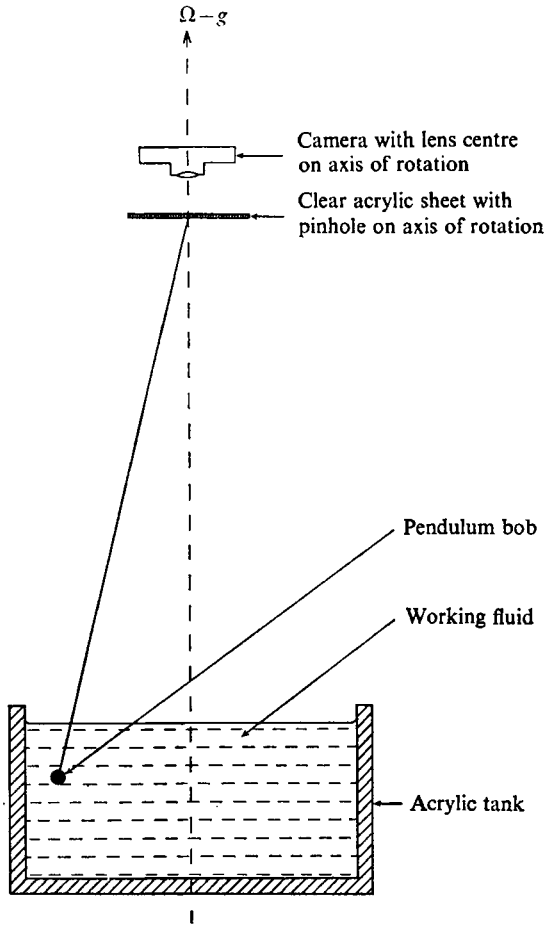


FIGURE 1. Schematic diagram of pendulum apparatus.

the experimental results are strikingly similar to the results of a theory which does not have obvious relevance to the experiments: Stewartson's (1953) theory for the force acting on an ellipsoid as it moves through an inviscid unbounded fluid at zero Rossby number agrees remarkably well with the experimental results for which a Taylor column did *not* form. No explanation is offered for this surprising quantitative agreement.

The pendulum experiment and its results are described in §§ 2.1 and 2.2 respectively and the spinning-disk experiment and its results are described in §§ 3.1 and 3.2 respectively.

## 2. The 'pendulum' experiment

### 2.1. *Apparatus and experimental method*

*Apparatus.* The apparatus used is schematically illustrated in figure 1. The object was suspended on a copper wire 0·005 cm in diameter from a rigid support mounted on a tripod attached to a turntable. The point of suspension was a fine

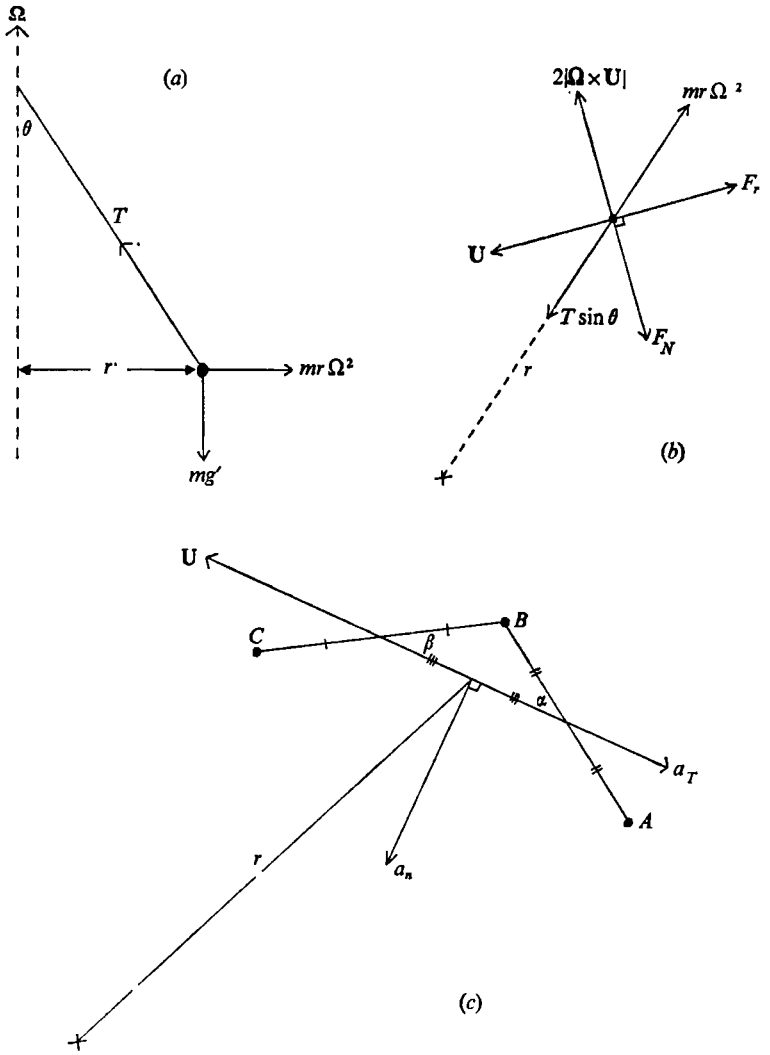


FIGURE 2. (*a*) Forces in the plane of the pendulum bob and the axis of rotation (any vertical forces due to the fluid have been neglected; see text). (*b*) Forces in a horizontal plane containing the pendulum bob. (*c*) Illustrating the method of calculation of the tangential and normal accelerations of the pendulum bob from the position of three images $A$, $B$ and $C$ each separated by a time interval $\Delta t$. The tangential acceleration $a_T = (AB\cos\alpha - BC\cos\beta)/\Delta t^2$ and the normal acceleration $a_N = (AB\sin\alpha + BC\sin\beta)/\Delta t^2$, where $\alpha$ and $\beta$ are defined such that they are negative angles when the line bisecting $CB$ and $BA$ lies to the right of the **U** direction at point $B$.

hole 0·01 cm in diameter in a clear acrylic sheet. This hole was positioned within 0·05 cm of the axis of rotation. The length $l$ of the pendulum formed by this arrangement was nominally 1 m and was measured to an accuracy of 1 mm by a cathetometer. The object was immersed in a fluid in a rectangular container 60 cm long, 30 cm wide and 30 cm deep which was mounted on the turntable beneath the tripod. The base and walls of the container deviated from the

horizontal and vertical by less than $2 \times 10^{-3}$ rad and the axis of rotation of the apparatus deviated from the vertical by less than $3 \times 10^{-4}$ rad.

The turntable was driven by a synchronous induction motor via a Graham continuously variable speed transmission unit. Typical values of $\Omega$ were 0·25–3 rad s$^{-1}$ and could be maintained constant to an accuracy of 0·1 % for periods of order 1 h. Individual rotation periods could be measured by means of an electronic timing unit actuated when a beam of light from a lamp fixed in the laboratory reflected by a plane mirror mounted on the turntable was intercepted by a fixed photo-resistor.

A 35 mm camera was mounted on the tripod attached to the turntable, with its lens centred on the axis of rotation, looking through the clear acrylic sheet from which the object was suspended (see figure 1). The object was painted black and a small white cross was drawn through the point of suspension. The base of the rectangular container was also painted black so the camera saw the object as a small white cross. The object was illuminated by means of a stroboscopic light source. Provided that the rotation rate $\Omega$ was not greater than $(g/l)^{\frac{1}{2}}$ ($g$ being the acceleration due to gravity) the equilibrium position of the pendulum was a point on the axis of rotation, and this position was recorded photographically.

*Experimental procedure.* In each experimental run the object was carefully drawn to one side by a horizontal rigid wire. It was held by this wire such that the weight of the object was borne by the suspending wire and the centre of mass of the object lay on the extrapolated line of the suspending wire. The object could then be released in a controlled manner by pulling aside the rigid wire. At the moment of release the camera shutter was opened and with the stroboscopic illumination the trajectory of the bob was recorded. From the resulting photographs the distance of each image from the axis of rotation and the distance between adjacent images were measured. Allowance for geometric distortion was made by photographing rules in the plane of movement of the object. From each set of three adjacent measurements of radius and two of image separation it is a simple matter to compute the forces $F_T$ and $F_N$ acting on the bob, and the method of calculation is illustrated by figures 2 (*a*)–(*c*). The vertical acceleration of the object is negligible compared with $mg'$ (see below) and the size of the vertical force experienced by a body falling axially through a rotating fluid can be deduced from previous experiments (Maxworthy 1970). For the range of parameters appropriate to the present experiments this force is $\sim 2\Omega\rho w V$, where $w$ is the vertical velocity of the object. In the present work this leads to a value of the force always very much less than $mg'$. The total errors in the measurement of the lengths were estimated to be $\pm$ 0·05 mm, and with the typical image separation ($\sim$ 1 cm) the total random errors in the value of force were about $\pm$ 20 %.

The parameter range of the measurements was varied by two methods: either the rotation rate was altered or the density of the fluid in which the objects were immersed was changed. The objects were made of Perspex (density $\rho_p$ = 1·35 g cm$^{-3}$). Thus in fluid of density $\rho$ the objects move under reduced gravity $g' = g(\rho_p - \rho)/\rho$. The basic fluid used was water and the changes in density were achieved by using salt (sodium chloride) solutions; concomitant changes in the kinematic viscosity were relatively small. Low Rossby number measurements

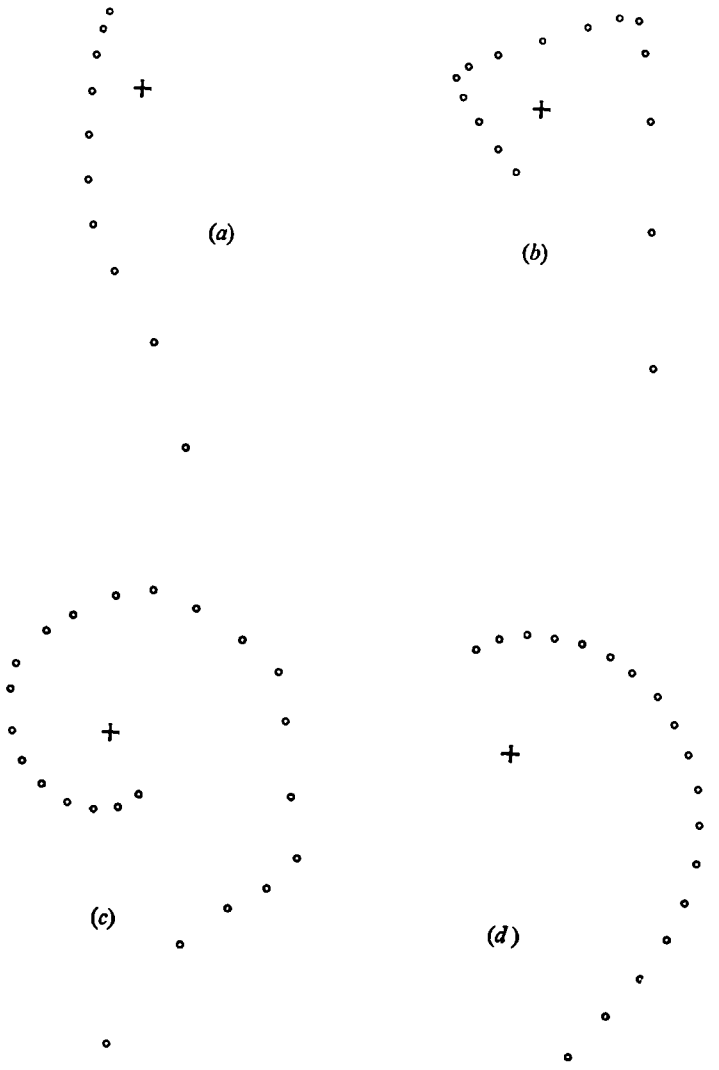


FIGURE 3. Illustrating the dependence of the trajectory of the bob on rotation rate. (*a*) $\Omega = 0$, flash interval = 0·27 s. (*b*) $\Omega = 0{\cdot}63\,\mathrm{rad\,s^{-1}}$, flash interval = 0·51 s. (*c*) $\Omega = 1{\cdot}25\,\mathrm{rad\,s^{-1}}$, flash interval = 0·71 s. (*d*) $\Omega = 2{\cdot}50\,\mathrm{rad\,s^{-1}}$, flash interval = 1·47 s. The curvature of the trajectory (*a*) at $\Omega = 0$ is due to asymmetric shedding of eddies. The cusps in the trajectories (*b*) and (*c*) at $\Omega = 0{\cdot}63$ and $1{\cdot}25\,\mathrm{rad\,s^{-1}}$ are due to inertial overshoot. The smooth trajectory (*d*) at $\Omega = 2{\cdot}50\,\mathrm{rad\,s^{-1}}$ is typical of one used for measurement.

were obtained with $(\rho_p - \rho)/\rho$ small and $\Omega$ large ($\sim 3\,\mathrm{rad\,s^{-1}}$). High Rossby number measurements were obtained with pure water as the fluid and $\Omega$ moderate ($\sim 1{\cdot}5\,\mathrm{rad\,s^{-1}}$). It was not possible to make accurate measurements at low $\Omega$ ($\sim 0{\cdot}5\,\mathrm{rad\,s^{-1}}$) because of the cusps (see figure 3) in the trajectory. These cusps were due to the relative importance, at low $\Omega$, of the inertia of the object and were not adequately recorded by the measurements.

*Limitations of experiment.* The forces on the objects in the range of Rossby numbers $10^{-2}$–1 are very small (of the order of dynes) and in a rotating frame

would be very difficult to measure directly. The present experiments provide a very simple method of measuring these forces but do have several inherent defects.

(*a*) Eddies are shed by objects and consequently the drag force varies with time. The method of measurement averages this effect to some degree but the remaining variations are typically 20 % of the mean drag and lead to some scatter in the experimental results.

(*b*) The data were intended to represent a steady-state drag, but clearly the bob was always accelerating to some degree. To minimize this effect the data were obtained from the central third of the trajectory between the point of release and the origin. Over this distance the speed was found (at the values of $\Omega$

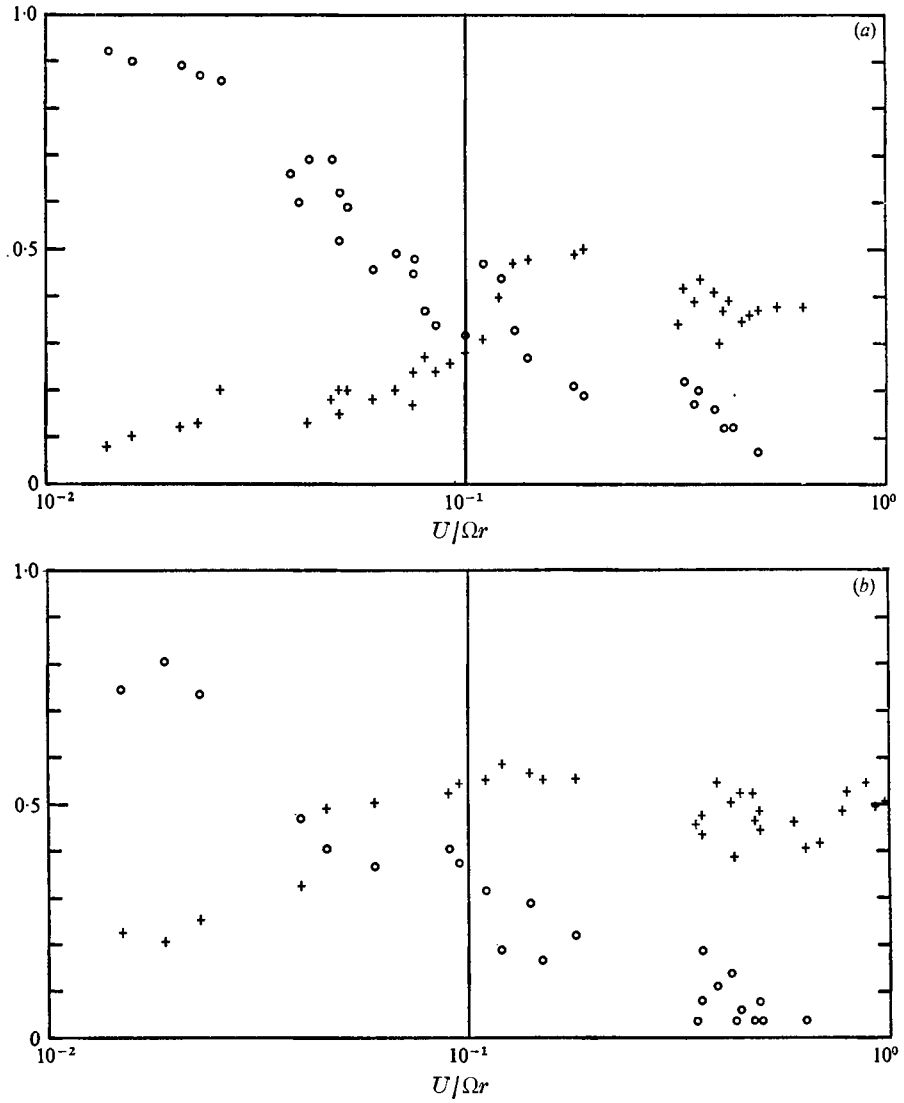


FIGURES 4 (*a*) and (*b*). For legend see opposite page.

used; see above) to vary by less than 20 % of its mean value. Indeed over this part of the trajectory the changes in the kinetic energy of the object were less than a few per cent of the changes in its potential energy. For $R \sim 1$ the apparatus performed about three revolutions between the time of release and time of arrival at the central third of the trajectory, and since the number of revolutions in this period is proportional to $R^{-1}$, for most of the data motion on the time scale $\Omega^{-1}$ must have been close to equilibrium.

(*c*) The upper surface of the fluid in which the object was immersed was free and thus, owing to the effects of rotation, was slightly parabolic in shape. This change in depth with radius led to a deflecting force on the object. An order-of-magnitude comparison between the characteristic length scales due to this force and that due to the Coriolis force, i.e. between $(U/\beta)^{\frac{1}{2}}$ and $U/\Omega$ (where $\beta = 2\Omega\theta/D$, $\theta$ is the slope of the free surface and $D$ is the depth of the fluid), shows that in the worst case $(U/\beta)^{\frac{1}{2}}$ was $\sim 3$ cm, compared with $U/\Omega \sim 0{\cdot}05$ cm, i.e. the forces due to the change of depth should have been negligible.

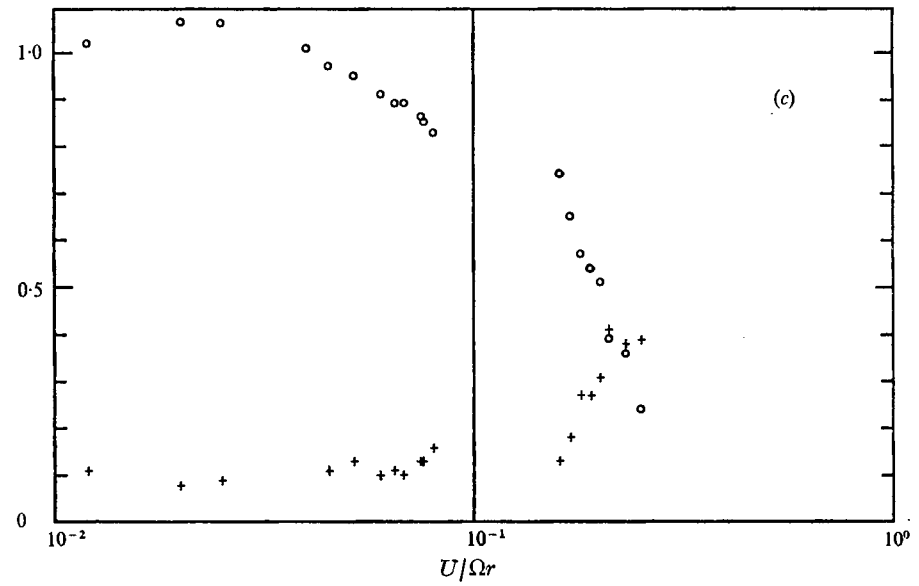


FIGURE 4. Experimental values of the drag ($F_T$) and lift ($F_N$) forces for different values of the Rossby number. The bob was a sphere. The working fluid varied between pure water and sodium chloride solution of density 1·2 g cm$^{-3}$. ○, $F_N/2\Omega\rho UV$; +, $F_T/2\Omega\rho UV$. (*a*) Bob radius = 1·85 cm, fluid depth = 18 cm. (*b*) Bob radius = 0·95 cm, fluid depth = 18 cm. (*c*) Bob radius = 1·85 cm, fluid depth = 8 cm.

### 2.2. *Results*

*Spheres.* Measurements were made, as described in § 2.1, of the force on spheres of varying size in fluids of varying depth. Figures 4 (*a*)–(*c*) show some typical results. The size of the sphere varies between figures 4 (*a*) and (*b*) and the depth of the fluid between figures 4 (*b*) and (*c*). The drag force $F_T$ and lift force $F_N$ are scaled in terms of $G$ and plotted against the Rossby number. The drag force decreases as the Rossby number decreases and it is evident that the value of the Rossby number

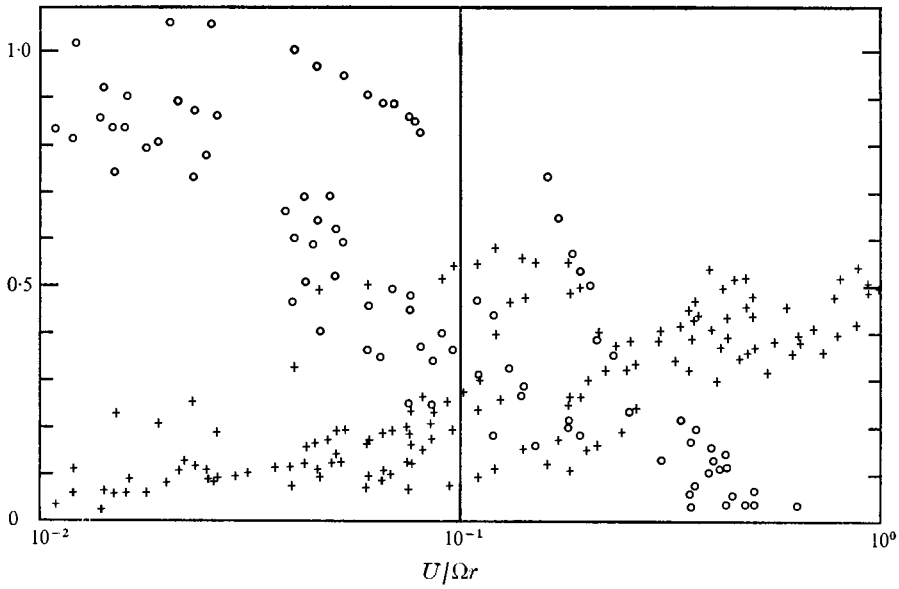


FIGURE 5. Experimental values of the drag ($F_T$) and lift ($F_N$) forces for different values of the Rossby number. This graph includes all the data for spherical bobs. The radius of the sphere was varied from 0·85 to 2·55 cm and the depth of the fluid from 8 to 18 cm. Symbols as in figure 4.

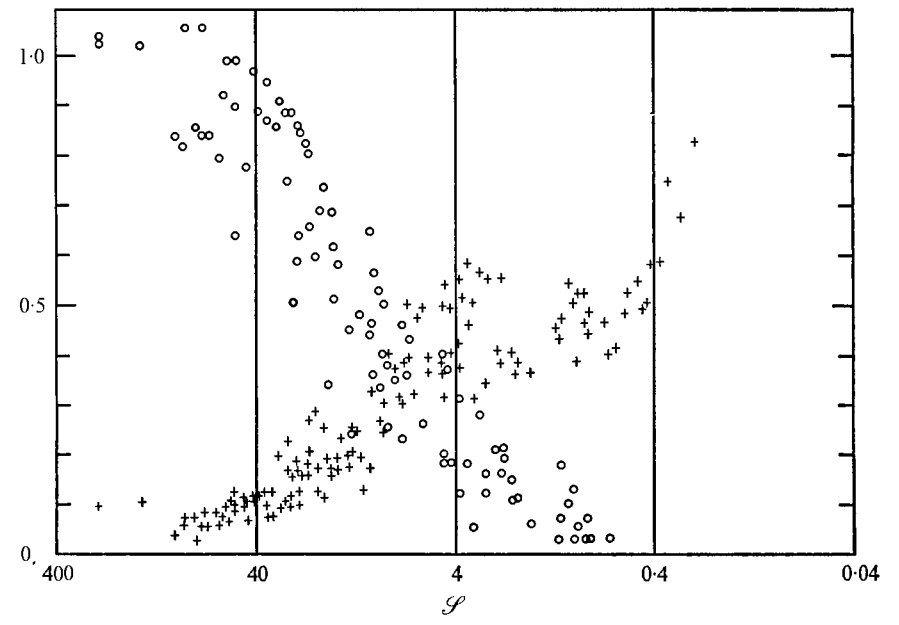


FIGURE 6. Experimental values of the drag ($F_T$) and lift ($F_N$) forces for different values of Hide's Taylor-column parameter $\mathscr{S} = 8\Omega r^2/DU$. The graph includes all the points shown in figure 4(*c*). Symbols as in figure 4.

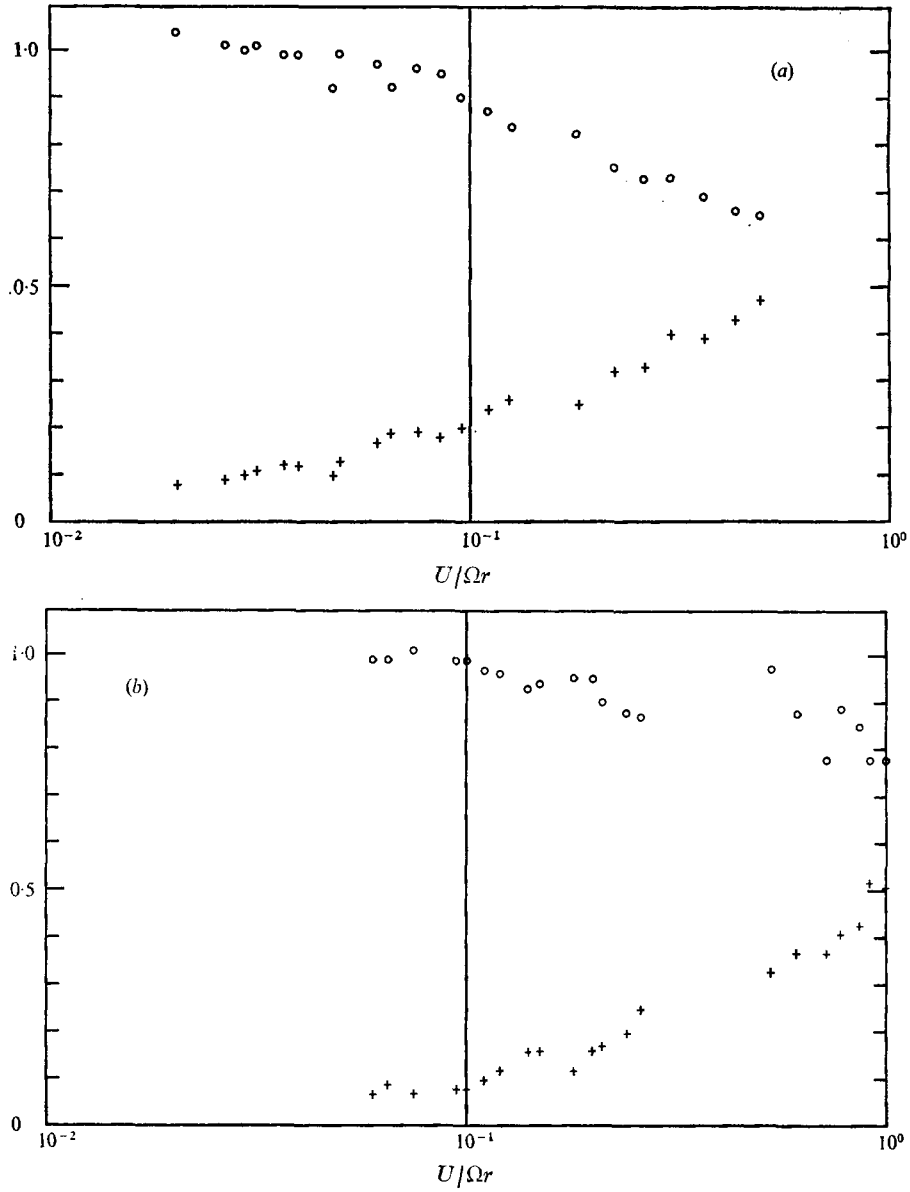


FIGURE 7. Experimental values of the drag ($F_T$) and lift ($F_N$) forces for different values of the Rossby number. The bob was a circular cylinder with spherical end caps. The depth of the fluid was 18 cm. The working fluid varied between pure water and sodium chloride solution of density 1·2 g cm$^{-3}$. (*a*) Cylinder radius = 1·20 cm, total height = 7·6 cm. (*b*) Cylinder radius = 0·36 cm, total height = 15 cm. Symbols as in figure 4.

at which the main decrease occurs depends upon both the size of the sphere and the depth of the fluid. At Rossby numbers less than unity, but higher than those corresponding to the main decrease in drag, the drag force is roughly constant at $\sim 0{\cdot}5G$. The size of the non-rotating drag force $\frac{1}{2}\rho A U^2$ is significant only for Rossby numbers greater than unity.

The lift force $F_N$ is close to zero for higher Rossby numbers but tends to $G$ as the Rossby number becomes small. As with the drag force, the values of the Rossby number for which the lift force changes are seen to depend on both the size of the sphere and the depth of the fluid.

In the experiments the radius of the sphere was varied from 0·95 to 2·55 cm and the depth $D$ of the fluid was varied from 8 to 18 cm. The data obtained from all these experiments are plotted against the Rossby number in figure 5. The considerable scatter should be compared with figure 6, in which the same data are plotted against Hide's Taylor-column parameter $\mathscr{S} = 8\Omega r^2/DU$. The scatter in figure 6 is much less and comparable with the experimental errors. For $\mathscr{S} < 1$ the lift force is small and in the range $\mathscr{S} = 1$–100 it increases to $G$. Visual observations in the present and previous (Hide & Ibbetson 1966) experiments indicate that this range $\mathscr{S} = 1$–100 corresponds to the formation of a Taylor column over the object. As the lift force increases, the drag force decreases and tends to a value that order-of-magnitude calculations show to be comparable with that due to Ekman layers.

*Cylinders.* A few experiments were carried out with objects of roughly spheroidal shape. Oblate objects were found to tilt their axes to and fro as they moved through the fluid. In consequence their motion was jerky and accurate measurements were impossible (cf. Stewartson 1954). Prolate objects moved smoothly and figures 7 (*a*) and (*b*) show measurements using cylinders with spherical caps. As the length of the cylinder approaches the depth of the fluid the results show a clear trend towards Taylor's two-dimensional result. The lift force increases towards $G$ whilst the drag force decreases towards the non-rotating value.

## 3. The spinning-disk experiment

### 3.1. *Apparatus and experimental method*

*Apparatus.* The apparatus is illustrated schematically in figure 8. A clear acrylic plastic cylinder of internal radius 14·00 cm was mounted on a turntable. The cylinder had a fixed base and contained two immiscible liquids. The lower layer (2·8 cm deep) was a nearly saturated solution of potassium iodide in water with density 1·65 g cm$^{-3}$. The upper layer (of depth $D = 19{\cdot}0$ cm) was paraffin (kerosene) with density 0·77 g cm$^{-3}$ and kinematic viscosity $\nu = 1{\cdot}39 \times 10^{-2}$ cm$^2$ s$^{-1}$. A plastic disk 1·8 cm thick and of radius 12·97 cm floated between these two liquids. An alloy disk of thickness 0·62 cm and radius $b = 13{\cdot}77$ cm was mounted on the output shaft of a motor and gearbox and suspended from the lid of the cylinder such that it lay below the upper surface of the paraffin layer. The objects were glued directly onto the underside of this disk. The axis of rotation of the turntable deviated from the vertical by less than $3 \times 10^{-4}$ rad and the base and wall of the Perspex cylinder deviated from the horizontal and vertical respectively by $2 \times 10^{-3}$ rad. The upper (alloy) disk was horizontal to within $10^{-3}$ rad and concentric with the inside of the Perspex cylinder to within 0·01 cm. The upper (alloy) disk was made to rotate slower than the turntable and thus drive the flow.

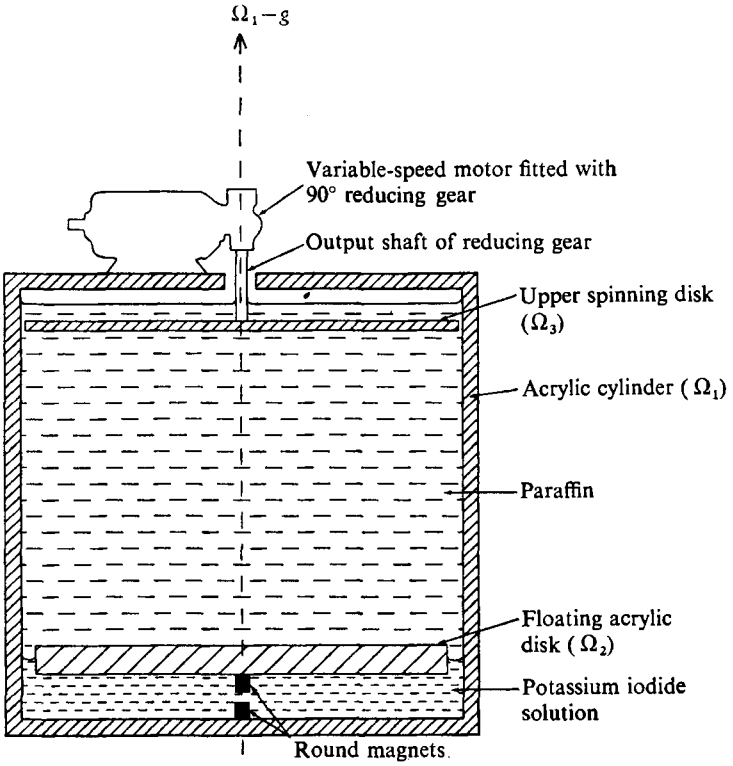


FIGURE 8. Schematic diagram of spinning-disk apparatus.

The turntable was driven by a synchronous induction motor via a Graham continuously variable speed transmission unit. The typical value of $\Omega$, the turntable's angular speed, was $2{\cdot}5\,\mathrm{rad\,s^{-1}}$ and could be maintained constant to within 0·1 % over periods of the order of 1 h. Individual rotation periods $2\pi/\Omega$ could be measured by means of the electronic timing unit mentioned in § 2.1. The rotation speeds relative to the turntable of the upper (alloy) disk and the floating (plastic) disk were measured in a similar way. The lamps and photo-resistors were mounted on the turntable and the plane mirror replaced by small pieces of reflective adhesive tape. In order to average out small fluctuations in the rotation speeds the electronic counter was set to measure ten rotation periods. The rotation periods of the turntable and upper spinning disk averaged over ten rotation periods were constant to within 0·025 %. The rotation period of the floating disk was constant to the same accuracy when no objects were attached to the upper spinning disk, but with objects attached it was slightly less constant.

For the purpose of the experiment it was essential that the floating disk remained in the centre of the cylinder and did not touch its sides. With no objects attached to the upper spinning disk the parabolic shape of the geopotentials was a sufficient constraint. With an object on the upper spinning disk a further constraint was found to be necessary: two round bar magnets with symmetrical fields were used (see figure 8). One magnet was mounted vertically at the centre of

the lower side of the floating disk whilst the other was mounted on the centre of the base of the tank. The attractive force between these magnets was found to reduce any sideways movements of the floating disk to less than 0·5 mm.

*Method of measurement.* The principle of the experiment is that the torque introduced into the fluid by the upper spinning disk must be communicated through the floating disk to the base of the apparatus. To communicate the torque the floating disk must also spin relative to the base and the magnitude of this spin is a measure of the torque transmitted. In order to make calculating the size of the torque tractable the parameters of the experiment were arranged such that the Ekman-layer dynamics dominated the flow, i.e. such that the Ekman-layer spin-up time scale $t_E = D/2(\Omega\nu)^{\frac{1}{2}}$ ($\sim$ 50 s here) was very much less than the viscous diffusion time scale $t_\nu = b^2/\nu$ ($\sim 1{\cdot}4 \times 10^4$ s here) and the Ekman number $\nu/\Omega D^2 \ll 1$ ($\sim 2 \times 10^{-5}$ here). For linear Ekman-layer equations to apply the Rossby number $\Delta\Omega/\Omega$, where $\Delta\Omega$ is the differential rotation of the fluid relative to the disk, must be less than $\sim$ 1 (a maximum of $\sim$ 0·15 here) (Greenspan 1968, §3). To calculate the torque the Ekman layers must also be stable, and the experiments of Tatro & Mollo-Christensen (1967) show that, for the Rossby numbers used in the present work, the Reynolds number $Re = \delta U/\nu$ (where $\delta$ is the Ekman-layer thickness $(\nu/\Omega)^{\frac{1}{2}}$) must be less than $\sim$ 75 for this to be so. The *largest* value of this Reynolds number in the present work was $\sim$ 50 and moreover flow visualization with aluminium powder showed the boundary layers to be free from such instability.

In order to avoid the difficult task of obtaining a complete theory for the flow in the apparatus a comparison was made between each experiment with an object and a null experiment without the object. In an experiment with an object the angular speeds $\Omega_1$, $\Omega_2$, and $\Omega_3$ of the turntable, floating disk and spinning disk respectively were measured. Then in the experiment without the object $\Omega_1$ was left unaltered and $\Omega_3$ adjusted to a new value $\Omega_3^*$ such that $\Omega_2$ had the same value as before. In practice with *no* object mounted the ratio $(\Omega_3^* - \Omega_1)/(\Omega_2 - \Omega_1)$ was found to be a constant and the latter experiment was a hypothetical one based on the constancy of this measured ratio. It is then clear that provided that the frictional coupling between the turntable and floating disk is unchanged the torque transmitted through the disk in the two cases is the same. The frictional coupling is dominated by Ekman suction between the floating disk and the base of the container and the long-term reproducibility of the experiments show it to be constant. We may thus equate the torque due to the object and spinning disk rotating at $\Omega_3$ with that due to the spinning disk alone at $\Omega_3^*$, i.e. the Ekman-layer system with differential rotation $\Omega_2 - \Omega_3^*$ transmits the same torque as the object/Ekman-layer system with differential rotation $\Omega_2 - \Omega_3$.

We can parameterize the effect of the object as an equivalent Ekman layer of thickness $\delta_B$, so that the disk to which the object is attached has an Ekman layer of total thickness $\delta + \delta_B$. Such a parameterization is especially natural in view of the results of the pendulum experiment, in which the drag force on an object was found, like the stress due to an Ekman layer, to be proportional to $U$. The experiment thus provides an accurate method of determining this parameterization of the effect of an object in the present system. It is clear that such

a study would show how $\delta_B$ depends on the shape of the object and thus serve as a guide to which length scales might comprise the volume $V$ in a geostrophic drag $\sim 2\rho\Omega U V$ when the object is not a sphere. In what follows an attempt is made to go further and use questionable assumptions to determine the force implied by a certain value of the equivalent Ekman-layer thickness $\delta_B$; in view of the agreement with the pendulum experiment and certain internal empirical checks the attempt appears successful.

The prototype of the problem we are considering is the flow due to a slow differential rotation of the upper and lower horizontal boundaries of a cylinder of rapidly rotating fluid (Stewartson 1957). For example, consider a container having a mean basic rotation speed $\Omega$ with the upper and lower surfaces rotating at $\Omega-\Delta\Omega$ and $\Omega+\Delta\Omega$ respectively. The interior region between horizontal Ekman layers of thickness $\delta = (\nu/\Omega)^{\frac{1}{2}}$ and vertical shear layers of thicknesses $(D^2\nu/\Omega)^{\frac{1}{4}}$ and $(D\nu/\Omega)^{\frac{1}{3}}$ is in rigid-body rotation at $\Omega$. The flow is controlled by the Ekman layers and the passive vertical shear layers serve only to permit return circulation and match horizontal velocity differences. This motion of the interior region relative to the boundaries develops balanced torques and mass fluxes in the Ekman layers with a vertical velocity uniform with height and of the same sign everywhere in the interior. The stress on a horizontal surface in the direction of **U**, where **U** is the flow above the Ekman layer on that surface, is

$$\tau_E = \rho\nu U/\delta. \tag{1}$$

It follows that the torque on a disk of radius $b$ spinning at $\Omega-\Delta\Omega$ relative to fluid rotating at $\Omega$ is

$$T = \tfrac{1}{2}\rho\delta\Omega\Delta\Omega b^4\pi. \tag{2}$$

To calculate the equivalent Ekman-layer thickness $\delta_B$ we note that to be consistent with parameterizing the effect of the object as an equivalent Ekman layer the interior flow in both the experiment with an object and the null experiment must be considered to be rigid-body rotation at the same speed. In the null experiment the upper and lower spinning disks rotate at $\Omega_3^*$ and $\Omega_2$, and we have an interior flow at $\frac{1}{2}(\Omega_3^*+\Omega_2)$. In the experiment with the object the balancing of Ekman torque between the upper Ekman layer, of thickness $\delta+\delta_B$, and the lower layer, of thickness $\delta$, implies an interior rotation at $[\delta\Omega_2+(\delta+\delta_B)\,\Omega_3]/(2\delta+\delta_B)$. We could equate these two interior speeds to obtain $\delta_B$, but anticipating equations below, we take the equivalent step of equating the torques entering the fluid from the upper disk in both experiments, i.e.

$$(\delta+\delta_B)\left(\frac{\delta\Omega_2+(\delta+\delta_B)\,\Omega_3}{2\delta+\delta_B}-\Omega_3\right) = \delta\left(\frac{\Omega_2+\Omega_3^*}{2}-\Omega_3^*\right). \tag{3}$$

Thus

$$\delta_B \equiv \frac{2\delta(\Omega_3-\Omega_3^*)}{\Omega_2+\Omega_3^*-2\Omega_3}. \tag{4}$$

Visual observations of the flow using a suspension of aluminium powder showed the objects (whose Reynolds numbers varied between about 100 and 3000) to be shedding eddies. This suggests that the retardation of the flow by the object will spread away from the location of the object and means that, with no theory for this spreading and other inevitable complications, we may calculate

the drag force only for circumstances under which the assumption that the interior region has a uniform regular velocity $\frac{1}{2}(\Omega_2+\Omega_3^*)$ leads to no significant error. This assumption is clearly never exactly true but we leave a discussion of its theoretical and empirical justification until after we have shown how the drag was calculated.

We are assuming that the interior flow is that taken for the purpose of defining an equivalent Ekman-layer thickness $\delta_B$. It follows that the torque due to the object in excess of that due to the Ekman layer on the upper disk is

$$T_B = \tfrac{1}{4}\rho\delta_B(\Omega_2+\Omega_3^*)[\tfrac{1}{2}(\Omega_2+\Omega_3^*)-\Omega_3]b^4\pi. \tag{5}$$

If the object is small enough to be regarded as all being at a radius $r$ the drag force on the object is

$$F_B = T_B/r. \tag{6}$$

The azimuthal flow impinging on the object is

$$U_B = [\tfrac{1}{2}(\Omega_2+\Omega_3^*)-\Omega_3]r. \tag{7}$$

Thus we may define a geostrophic drag coefficient

$$E = F_B/(\Omega_2+\Omega_3^*)\,U_B\rho V, \tag{8}$$

where $V$ is the volume of the object. Then, using (5)–(8), we obtain

$$E = \delta_B\left(\frac{b^4\pi}{4Vr^2}\right) = \frac{\text{volume of equivalent Ekman layer}}{\text{volume of object}}\left(\frac{b^2}{4r^2}\right). \tag{9}$$

The essential justification for this calculation is empirical and no complete theoretical justification is attempted. The following discussion is merely intended to make the calculation plausible and does not constitute a proof of its validity.

First, we note the possibility that the turbulence produced by the object might affect the assumption of ordinary Ekman layers dominating the flow. Visual observations using an aluminium suspension showed that the smallest length scale appeared to be larger than the Ekman-layer thickness $\delta$ and pessimistic order-of-magnitude calculations (Landau & Lifshitz 1963, §§ 32, 33) based on the energy input implied by the force on the object and internal viscous dissipation confirm that the turbulence should be quite negligible on the length scale $\delta$. Similar calculations of eddy viscosity are more uncertain but indicate that the turbulence should not cause a significant viscous coupling of the fluid to the side walls. This view is also supported by the visual observations, which indicated that the turbulence was confined to the neighbourhood of the object.

Second, we consider the effect of any vertical variation in the interior flow; such variations are strongly inhibited by the constraint of rotation but because of difficulties in assigning values to appropriate length and velocity scales it is not obvious from order-of-magnitude calculations that they will be negligible. We thus note without giving a detailed proof that any vertical variation in interior speed which leads to the flow being less near the object than elsewhere will cause the calculated value of $E$ to be an underestimate of the value based on a knowledge of the true flow. To illustrate this we can consider an interior rotation

$\Omega_I[1+\epsilon z(\Omega_2-\Omega_3)]$, where $z$ varies between $\pm\frac{1}{2}$ between the upper and floating disks. If we then introduce a new equivalent Ekman-layer thickness $\delta_B^*$ balancing torques in and out of the fluid gives

$$(\delta+\delta_B^*)\{[\Omega_I-\tfrac{1}{2}\epsilon(\Omega_2-\Omega_3)]-\Omega_3\}=\delta\{\Omega_2-[\Omega_I+\tfrac{1}{2}\epsilon(\Omega_2-\Omega_3)]\} \tag{10}$$

and comparison with the null experiment [cf. equation (3)] gives

$$(\delta+\delta_B^*)\{[\Omega_I-\tfrac{1}{2}\epsilon(\Omega_2-\Omega_3)]-\Omega_3\}=\delta[\tfrac{1}{2}(\Omega_2+\Omega_3^*)-\Omega_3^*]. \tag{11}$$

If we follow through steps equivalent to those in (4)–(8) we obtain a new value for $E$, say

$$E^*=\delta_B^*(b^4\pi/4Vr^2), \tag{12}$$

and comparison of (3) and (11) gives a relationship between values of $\delta_B$ and $\delta_B^*$ for the same values of $\Omega_1$, $\Omega_2$, $\Omega_3$ and $\Omega_3^*$, namely

$$\frac{1+\delta_B/\delta}{2+\delta_B/\delta}=(1-\epsilon)\frac{1+\delta_B^*/\delta}{2+\delta_B^*/\delta}. \tag{13}$$

This shows that for differences between $\delta_B$ and $\delta_B^*$ to be less than 20% of $\delta_B$ with $\delta_B/\delta$ in the range 0·1–2 (see below) $\epsilon$ must be less than $\sim 0{\cdot}02$.

Last, we consider the consequences of the object only affecting the flow over a limited radial extent comparable with its own width. To obtain a feeling for how this might affect the calculations of $E$ we consider a hypothetical system in which the object only influences an annular fraction $\alpha$ of the container. In this fraction we consider a model of the flow similar to that proposed for the whole system, and we define a new equivalent Ekman thickness $\delta'_B$ to occur in this region. It follows that the speed of angular rotation $\Omega'$ in the interior of region $\alpha$ required to balance torques is given by

$$(\delta+\delta'_B/\alpha)/(\Omega'-\Omega_3)=\delta(\Omega_2-\Omega_3) \tag{14}$$

and in place of (3) we have

$$\tfrac{1}{2}\delta(1-\alpha)(\Omega_2-\Omega_3)+\alpha(\delta+\delta'_B/\alpha)(\Omega'-\Omega_3)=\delta[\tfrac{1}{2}(\Omega_2+\Omega_3^*)-\Omega_3^*]. \tag{15}$$

We may then follow through steps equivalent to (4)–(8) and obtain a new value for $E$, say

$$E'=\delta'_B(b^4\pi/4Vr^2). \tag{16}$$

The relationship between $\delta_B$ and $\delta'_B$ for the given values of $\Omega_1$, $\Omega_2$, $\Omega_3$ and $\Omega_3^*$ obtained by comparing (3) and (15) is

$$\frac{1+\delta_B/\delta}{2+\delta_B/\delta}=\frac{(1-\alpha)}{2}+\frac{\alpha(\alpha+\delta'_B/\delta)}{2\alpha+\delta'_B/\delta}. \tag{17}$$

We may now ask how large $\alpha$ must be for the difference between $\delta_B$ and $\delta'_B$ to be less than 20% of $\delta_B$. We find that, for $\delta_B/\delta=0{\cdot}1$, 0·5 and 2, $\alpha$ must be greater than 0·23, 0·60 and 0·85 respectively.

For any reasonable model of the interior flow the assumptions made in calculating $E$ imply the maximum possible flow speed impinging on the object consistent with communication of the torque to the floating disk via Ekman layers.

This means that the value of $E$ we calculate should always be an underestimate, and gives extra weight to the empirical checks on the results by suggesting that the correct result is unlikely to be a fortuitous consequence of cancelling errors. The experiments have not established the full range of parameter space over which meaningful calculations of $E$ may be made but have had the limited objective of operating in a window of parameter space for which the pendulum experiment indicated a geostrophic drag force with which the data could be compared, i.e. $R \sim 0{\cdot}5$–$0{\cdot}1$, $\mathscr{S} < 1$.

Apart from the above assumptions there are errors in $\delta_B$ and hence $E$ due to uncertainties in the measured rotation periods. These lead to errors of $\pm 20\,\%$ for $\delta_B/\delta$ in range 0·18–1 which increase as $\delta_B/\delta$ decreases or increases outside this range, and reach, for example, $\pm 32\,\%$ at $\delta_B/\delta = 0{\cdot}1$ and $\delta_B/\delta = 2$. For this reason data for $\delta_B/\delta < 0{\cdot}1$ and $\delta_B/\delta > 2$ were discarded and the errors from this source can be taken as typically $\pm 20\,\%$, which corresponds to the observed reproducibility of values of $\delta_B$.

We are now in a position to comment on the empirical justification for the method of calculating $E$. When the spheres used in the pendulum experiment were glued directly onto the lower surface of the upper disk at about the mid-radius the values of $E$ obtained agreed with those obtained in the pendulum experiment to within $\pm 20\,\%$. Also, provided that the objects did not extend to within 1 cm of the edge of the disk, which would have brought them into the side-wall boundary layers, the values of $E$, but not of course $\delta_B$, were found to be independent of the radius at which the object was placed. This result is more than a spot check and, in view of the above discussion, the independence of the values of $E$ of the absolute size of the objects is of importance in indicating that the assumptions are substantially correct. In view of the discussion it is of particular importance that the effect of more than one object on $\delta_B$ was found to be additive provided that the objects were more than 30° downstream of each other.

In the case of objects which are not spherical in shape this empirical check could be regarded as inadequate. However, even for these objects the values of $E$ are found to be independent of the absolute size of the objects and the effect of more than one such object on $\delta_B$ additive (mounted 90 or 180° apart). If the above discussion is qualitatively correct this result implies that the values of $E$ obtained are substantially correct and from the accuracy to which the effect of more than one object produces an additive effect on $\delta_B$ ($\sim 20\,\%$) we can deduce the implied accuracy of the assumptions. We assume that the interior flow with an object on the upper disk is a rigid-body rotation at $\frac{1}{2}(\Omega_2 + \Omega_3^*)$. The errors in this value of $\frac{1}{2}(\Omega_2 + \Omega_3^*)$ can be no larger than $\sim 5\,\%$ of $\Omega_2 - \Omega_3$. The assumptions are only intended to be reasonable in the present context and it should be emphasized that the flow is not, and could not be expected to be, *exactly* as it has been assumed.

### 3.2. *Results*

*The effect of varying the horizontal aspect ratio.* Preliminary experiments showed that cubes produced values of $E$ which did not significantly differ from those for spheres of the same volume and consequently it was decided to avoid the expense

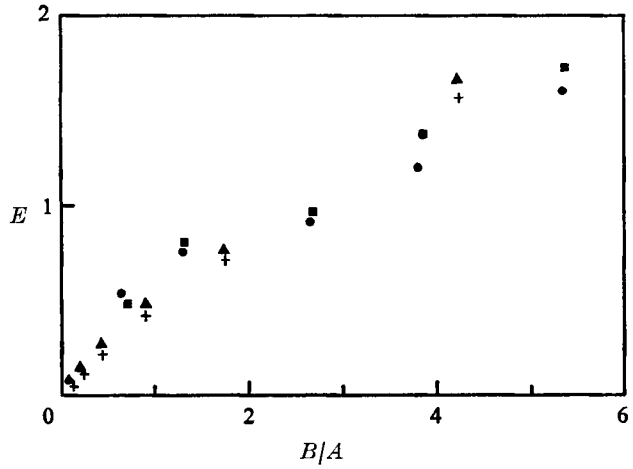


FIGURE 9. Illustrating the dependence of the geostrophic drag coefficient $E$ on the horizontal aspect ratio $B/A$ of the object. The height of the object $C = 2{\cdot}5$ cm. ▲, +, $B \approx 2$ cm, varying $A$; ■, ●, $A \approx 2$ cm, varying $B$. $\Omega_1 = 2{\cdot}5\,\mathrm{rad\,s^{-1}}$. ▲, ■, $\Omega_1 - \Omega_3 = \frac{2}{5}\pi\,\mathrm{rad\,s^{-1}}$; +, ●, $\Omega_1 - \Omega_3 = \frac{2}{10}\pi\,\mathrm{rad\,s^{-1}}$.

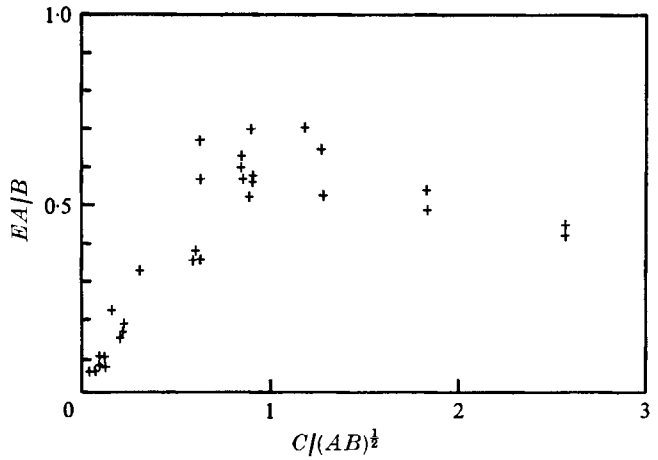


FIGURE 10. Illustrating the dependence of the geostrophic drag coefficient $E$ on the vertical aspect ratio $C/(AB)^{\frac{1}{2}}$ of the object. The graph includes data in which $A$, $B$ and $C$ are all varied independently of each other. The dependence of $E$ on $B/A$ has been corrected for in accordance with the results in figure 9.

of obtaining ellipsoids. The objects used in the experiments were parts of annular rings of height $C$, radial width $B$, and mean arc length $A$, such shapes being preferable to cuboids in view of the circular nature of the basic flow. Each piece of annular ring was mounted 'concentrically' on the upper disk to within $\pm 0{\cdot}025$ cm. In order to investigate the dependence of $E$ on the ratio $B/A$ two experiments were carried out. In one $B$ was fixed and $A$ varied, and in the other $A$ fixed and $B$ varied. These experiments were carried out at two values of the Rossby number. The higher value was chosen such that the non-rotating force $\frac{1}{2}\rho A U^2$ was less than 10% of $2\Omega\rho U V$, i.e. $\Omega_3 - \Omega_1 = \frac{2}{5}\pi\,\mathrm{rad\,s^{-1}}$, and the lower

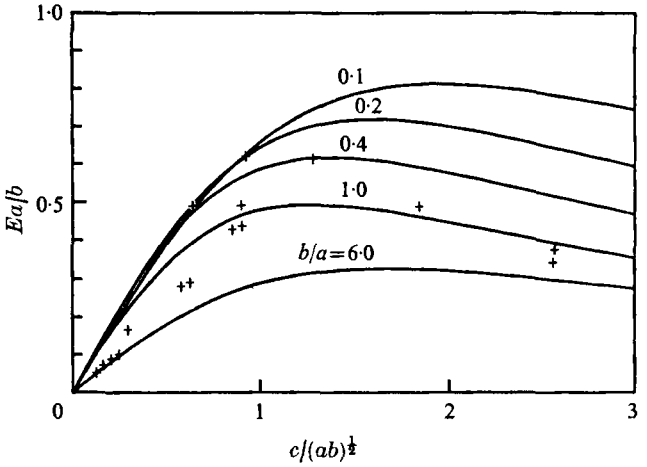


FIGURE 11. Curves of the geostrophic drag coefficient $Ea/b$ based on Stewartson's (1953) theory for the force on an ellipsoid moving transversely through a rotating fluid. $a$, $b$ and $c$ are the half-axes of the ellipsoid. The crosses are meant to indicate the values of $Ea/b$ expected in the experiments; they are positioned such that the aspect ratios of the ellipsoids in the theory correspond to the aspect ratios of the cuboids used in the experiments.

value was chosen such that Hide's Taylor-column parameter $\mathscr{S}$ was less than 0·1, i.e. $\Omega_3 - \Omega_1 = \frac{2}{10}\pi$ rad s$^{-1}$. The results of all these measurements are displayed in figure 9. The values of $E$ are seen to be roughly proportional to the ratio $B/A$ and roughly independent of both the Rossby number and the absolute values of $A$ and $B$. Some of the scatter is due to random errors but some may be due to a slight dependence on Rossby number; by holding $\Omega_3 - \Omega_1$ fixed the Rossby number of the flow is only maintained nominally constant. This result implies that the drag forces do not depend on the volume of the object, i.e. $ABC$, but on $B^2C$, i.e. they are nearly independent of $A$.

*The effect of varying the vertical aspect ratio.* If the data are required to be free of Taylor-column formation, i.e. $\mathscr{S} < 1$, and also meet the requirements of the calculation then it is not possible simply to choose a single value of $B/A$ and vary the height of the object over a large range. Instead, for a number of values of $B/A$, $C$ was varied as far as it could be and in order to prevent the variation of $B/A$ confusing the results the values of $EA/B$ are plotted against $C/(AB)^{\frac{1}{2}}$ in figure 10. The data are seen to be gathered together close to a single curve with a scatter of $\pm$ 0·1 in $EA/B$. The curve rises from zero for small $C/(AB)^{\frac{1}{2}}$ to a value of about 0·6 for $C/(AB)^{\frac{1}{2}} \sim 1$. For large $C/(AB)^{\frac{1}{2}}$ there is evidence of a decrease.

*Comparison with Stewartson* (1953). The theory of Stewartson (1953) gives values for the forces on an ellipsoid of volume $V$ and axes $a$, $b$ and $c$ moving through an unbounded inviscid rotating fluid at zero Rossby number. The drag forces from the theory are scaled in the same way as in the experiments and plotted against $c/(ab)^{\frac{1}{2}}$ in figure 11. The drag depends on $a/b$ and curves are plotted for $a/b$ varying from 6·0 to 0·10. To facilitate a comparison with the experiments points have been placed on this graph which correspond to the values of $A/B$ and $C/(AB)^{\frac{1}{2}}$ used in the experiments, i.e. such that $A/B = a/b$ and $C/(AB)^{\frac{1}{2}} = c/(ab)^{\frac{1}{2}}$.

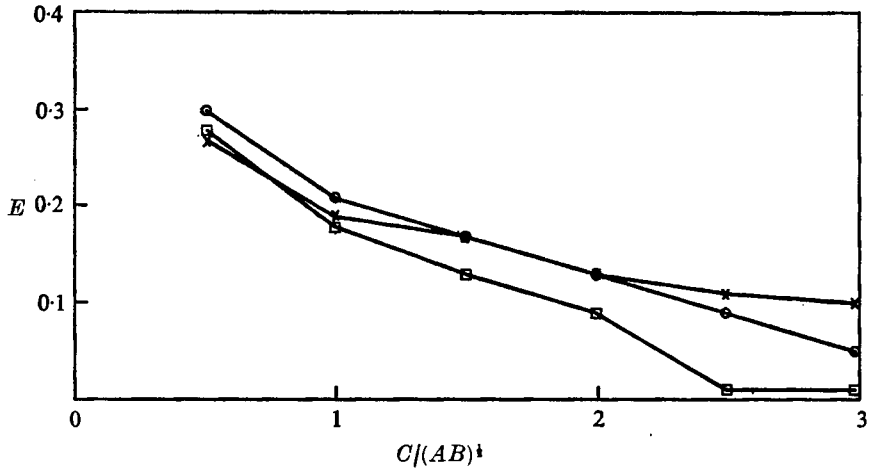


FIGURE 12. Illustrating the effect of Taylor-column formation on the geostrophic drag coefficient $E$. The height $C$ of an object with $A = B = 2{\cdot}5$ cm has been increased. Experimental details: $\Omega_1 = 2{\cdot}5\,\mathrm{rad\,s^{-1}}$; ×, $(\Omega_1 - \Omega_3)/\Omega_1 = 0{\cdot}5$, ○, $(\Omega_1 - \Omega_3)/\Omega_1 = 0{\cdot}25$; □, $(\Omega_1 - \Omega_3)/\Omega_1 = 0{\cdot}125$. The formation of Taylor columns leads to dependence of the goestrophic drag coefficient on Rossby number, i.e. $(\Omega_1 - \Omega_3)/\Omega_1$ (see also figure 13).

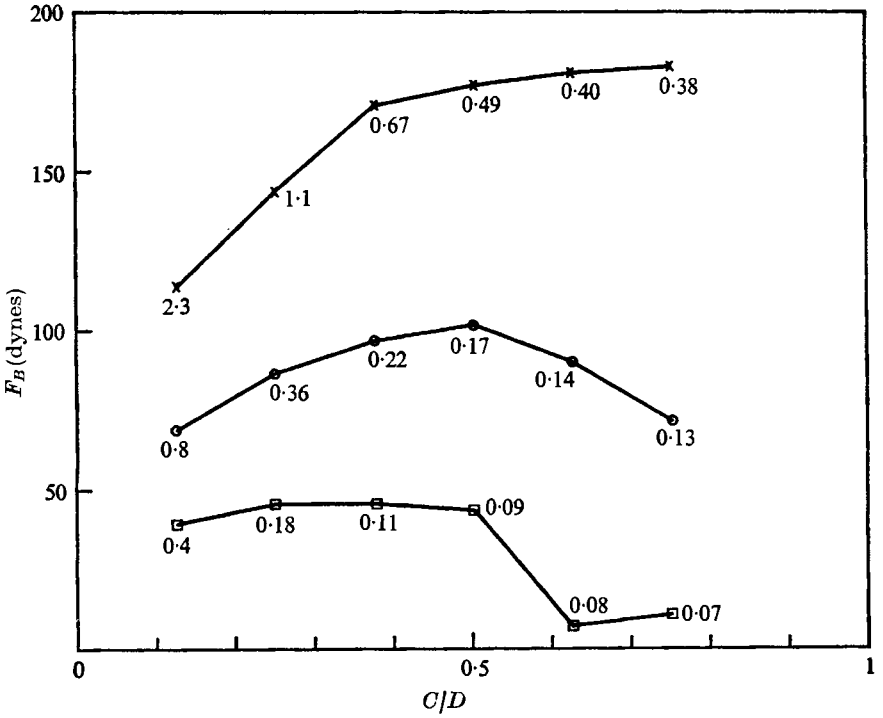


FIGURE 13. Illustrating the effect of Taylor-column formation on the drag force on an object. The height $C$ of an object with $A = B = 2{\cdot}5$ cm has been increased; apart from Taylor-column formation the drag force would be expected to increase roughly linearly with $C/D$. The observed decrease is a striking indication of the consequences of Taylor-column formation. Experimental details: $\Omega_1 = 2{\cdot}5\,\mathrm{rad\,s^{-1}}$; ×, $(\Omega_1 - \Omega_3)/\Omega_1 = 0{\cdot}5$; ○, $(\Omega_1 - \Omega_3)/\Omega_1 = 0{\cdot}28$; □, $(\Omega_1 - \Omega_3)/\Omega_1 = 0{\cdot}125$. Values of the reciprocal of Hide's Taylor-column parameter $\mathscr{S} = 8\Omega(AB)^{\frac{1}{2}}/DU$ are given alongside each point.

The distribution of these points in figure 11 may be compared with figure 10. It may be seen that, although there are differences of up to 50 % between the experiments and the theory, there is on the whole a striking qualitative agreement. As mentioned earlier, no explanation is given for this striking result, and following Greenspan (1968, p. 175) it may be worth noting that "This similarity of a distinctly non-linear motion and the limiting flow as $t \to \infty$ of a linear theory is probably accidental".

*Taylor columns.* The lowest Rossby numbers at which measurements can be made is governed by the stability of the turntable. Here (see §3.1) the stability of the turntable is 0·1 or 0·025 % depending on whether the rotation period is measured over 1 or 10 periods respectively. The smallest value of $(\Omega_3 - \Omega_1)/\Omega_1$ used was 0·125 as for smaller values the turntable fluctuations would have caused unacceptably large errors.

To illustrate the formation of a Taylor column the height $C$ of an object with $A = B$ was increased for three values of $(\Omega_3 - \Omega_1)/\Omega_1$, 0·5, 0·25 and 0·125. The results are shown in figures 12 and 13. Figure 12 shows the results as they would appear on figure 10; for the large values of $C/(AB)^{\frac{1}{2}}$ and small Rossby numbers the scaled force is seen to fall off rapidly. For comparison figure 13 shows the unscaled data; it is evident that the force is a maximum before the Taylor column forms. Values of the Taylor-column parameter $\mathscr{S}^{-1}$ are indicated against the points on figure 13. In agreement with the results of the pendulum experiment, the scaled drag falls for $\mathscr{S}$ in the range 2–12.

The author wishes to thank Mr D. Moore for his care in conducting the laboratory experiments and Dr R. Hide for the interest and support he gave to this work. This paper is published by permission of the Director-General of the Meteorological Office.

## REFERENCES

Davies, P. A. 1972 Experiments on Taylor columns in rotating stratified fluids. *J. Fluid Mech.* **54**, 691–717.

Grace, S. F. 1926 On the motion of a sphere in a rotating liquid. *Proc. Roy. Soc.* A **113**, 46–77.

Greenspan, H. P. 1968 *The Theory of Rotating Fluids.* Cambridge University Press.

Hide, R. 1961 Origin of Jupiter's great Red Spot. *Nature*, **190**, 213–218.

Hide, R. & Ibbetson, A. 1966 An experimental study of 'Taylor columns'. *Icarus*, **5**, 279–290.

Hide, R., Ibbetson, A. & Lighthill, M. J. 1968 On slow transverse flow past obstacles in a rapidly rotating fluid. *J. Fluid Mech.* **32**, 251–272.

Jacobs, S. J. 1964 The Taylor column problem. *J. Fluid Mech.* **20**, 581–591.

Landau, L. D. & Lifshitz, E. M. 1963 *Fluid Mechanics.* Pergamon.

Maxworthy, T. 1970 The flow created by a sphere moving along the axis of a rotating, slightly-viscous fluid. *J. Fluid Mech.* **40**, 453–479.

Moore, D. W. & Saffman, P. G. 1969 The flow induced by the transverse motion of a thin disk in its own plane through a contained rapidly rotating viscous liquid. *J. Fluid Mech.* **39**, 831–847.

Proudman, J. 1916 On the motions of solids in a liquid possessing vorticity. *Proc. Roy. Soc.* A **92**, 408–424.

STEWARTSON, K. 1953 On the slow motion of an ellipsoid in a rotating fluid. *Quart. J. Mech. Appl. Math.* **6**, 141–162.

STEWARTSON, K. 1954 On the free motion of an ellipsoid in a rotating fluid. *Quart. J. Mech. Appl. Math.* **7**, 231–246.

STEWARTSON, K. 1957 On almost rigid rotation. *J. Fluid Mech.* **3**, 17–26.

STEWARTSON, K. 1967 On slow transverse motion of a sphere through a rotating fluid. *J. Fluid Mech.* **30**, 357–369.

TATRO, P. R. & MOLLO-CHRISTENSEN, E. L. 1967 Experiments on Ekman layer instability. *J. Fluid Mech.* **28**, 531–544.

TAYLOR, G. I. 1923 Experiments on the motion of solid bodies in rotating fluids. *Proc. Roy. Soc.* A **104**, 213–218.

VAZIRI, A. & BOYER, D. C. 1971 Rotating flow over shallow topographies. *J. Fluid Mech.* **50**, 79–95.

WILCOX, D. C. 1972 The motion of a plate in a rotating fluid at an arbitrary angle of attack. *J. Fluid Mech.* **56**, 221–249.